Momentum Distribution and Effective Mass of Jellium and Simple Metals

Markus Holzmann

LPTMC, CNRS, Universite Pierre et Marie Curie, Paris

LPMMC, CNRS, Université Joseph Fourier, Grenoble, France

- QMC: Variational wave functions, imaginary time projection
  Finite Size Corrections

- Spectral properties (2DEG): Single-particle: $n(k)$, Z, and m^*
  Density fluctuations: $S(k,\tau)$, ω_p

- 3DEG, Na: Compton profile, $n(k)$, and Z

Ground state energies and wavefunctions for homogeneous (extended) Fermi systems (T=0)

- Variational principle for ground state of a finite system:

Hamiltonian for N non-relativistic Fermions:

$$H = \sum_{i=1}^{N} \left[-\frac{\hbar^2 \nabla_i^2}{2m} \right] + \sum_{i<j} V(\mathbf{r}_i - \mathbf{r}_j)$$

ground state energy E_0:

$$E_0(N) \leq E_T(N) \equiv \frac{\langle \psi_T | H | \psi_T \rangle}{\langle \psi_T | \psi_T \rangle}$$

Improve many-body trial wavefunctions $\Psi_T(\mathbf{r}_1, \mathbf{r}_2, \ldots, \mathbf{r}_N)$

- include explicit many body correlations in functional form
- stochastic improvement via Projector Monte Carlo (DMC,...) (fixed node approximation to avoid sign problem)

- Thermodynamic limit: $E_T(N) \to E_T(\infty)$?

- more general observables:

momentum distribution:

$$n_k \sim \int d\mathbf{r}_1 \int d\mathbf{r}'_1 e^{i\mathbf{k}\cdot(\mathbf{r}_1 - \mathbf{r}'_1)} \Psi_T^*(\mathbf{r}'_1, \ldots \mathbf{r}_N) \Psi_T(\mathbf{r}_1, \ldots \mathbf{r}_N)$$

- Excitation-energies (m*...)
- Dynamical correlations (S(k,ω), energy loss ...)

Many-body trial wavefunctions for Fermi systems

$$\psi_T(R) = A(R) \exp[-U(R)] \qquad R \equiv \{r_1, r_2, \ldots, r_N\}$$

Antisymmetric part:

determinant of single particle orbitals

$A(R)=\det_{ki}\, \varphi_k(r_i)$

orbitals must be plane waves (homogeneity)

→ Fermi liquid structure $k \leq k_F$

single particle excitations $k > k_F$

Symmetric correlations:

Jastrow potential:

$$U(R) = \sum_{i<j} u(r_{ij}) \qquad r_{ij} = |r_i - r_j|$$

$$= \frac{1}{2} \sum_k u_k \rho_k \rho_{-k} \qquad \rho_k = \sum_j e^{ikr_j}$$

→ electronic screening

collective excitations (plasmon)

improvements using backflow and many-body correlations

M. Lee, K. Schmidt, M.Kalos, and G.Chester, Phys. Rev. Lett. 46, 728 (1981).

M. H, D.M. Ceperley, C. Pierleoni, and K. Esler, Phys. Rev. E **68**, 046707 (2003)

M.H., B. Bernu, D. Ceperley Phys. Rev. B **74**, 104510 (2006)

Exact calculations for finite systems (N≈50-100)

(2DEG: homogeneous electron gas in 2D)

use exact projection in imaginary time (no fixed-node): $\Psi(\beta) = \exp[-\beta H]\Psi_T$

with different trial wavefunctions to estimate precision

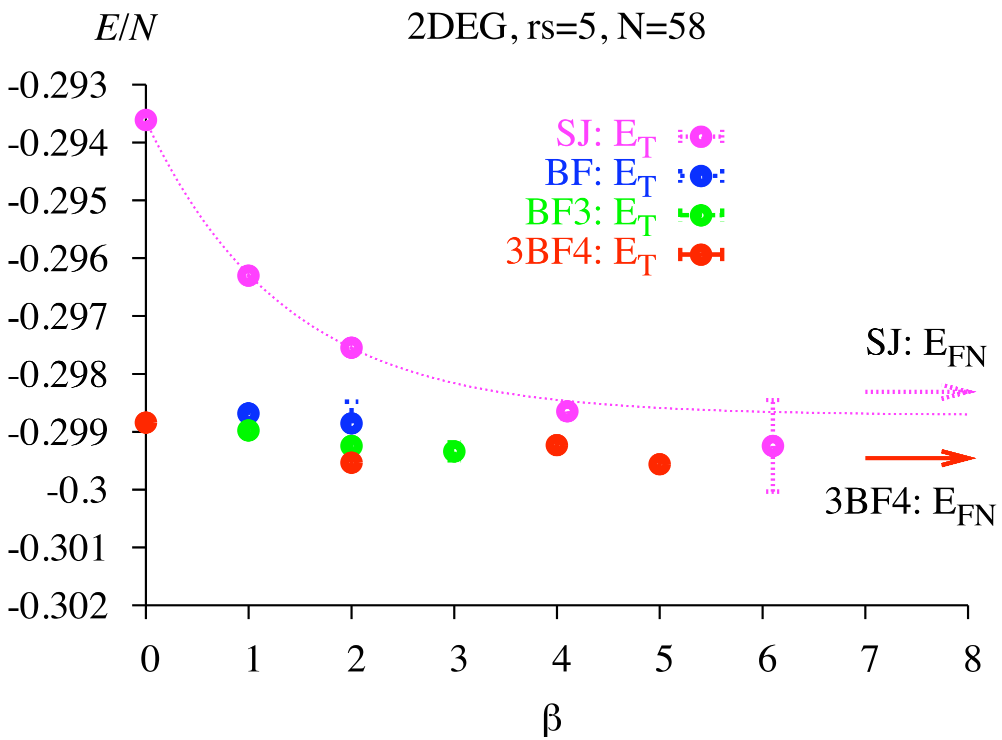

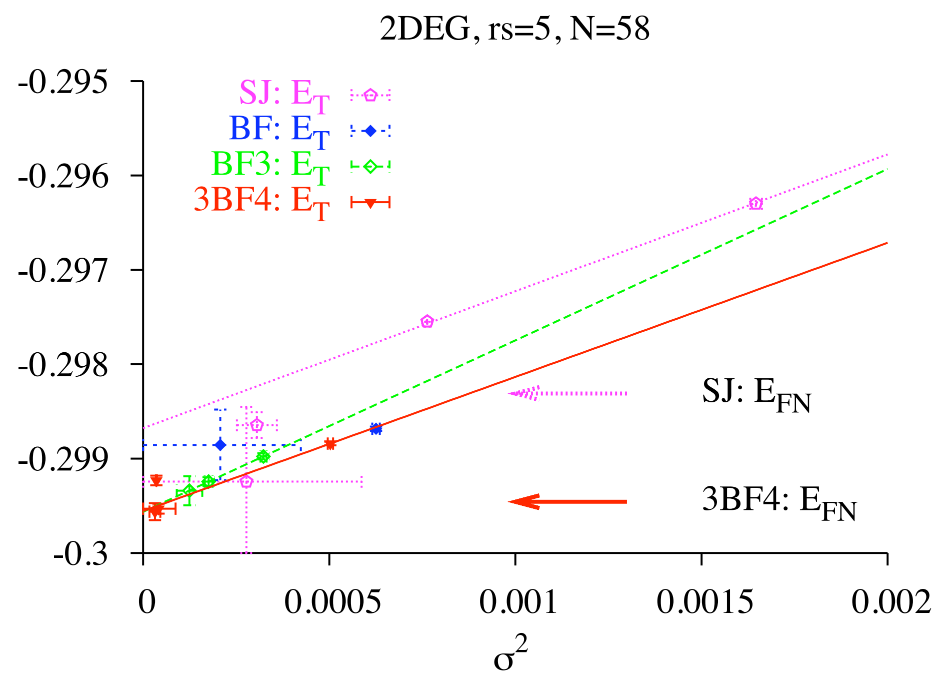

- **fixed node approximation:**
  - numerically stable evaluation of $\Psi(\beta) = \exp\left[-\beta H_{FN}\right]\Psi_T$
  - fixed node energies variational

Thermodynamic limit extrapolation: Energies

S. Chiesa, D.M. Ceperley, R.M. Martin, and M. H., Phys. Rev. Lett. **97**, 076404 (2006)

phenomenological: extrapolate always bigger systems with PBC...

E(L), E(2L), E(4L),..., => E(∞) L: size of system

or:

$$E(L) = \sum_k \frac{k^2}{2m} n_k^L + \sum_k v(k)[S^L(k) - 1]$$

$$\Downarrow$$

$$\frac{E(\infty)}{V} = \int \frac{d^D k}{(2\pi)^D} \frac{k^2}{2m} n_k^\infty + \int \frac{d^D k}{(2\pi)^D} v(k)[S^\infty(k) - 1]$$

→ finite size errors are integration errors

→ singularities/non-analytic points dominate size errors

Thermodynamic limit extrapolation: Potential Energy - Coulomb singularity (3D)

- Coulomb-potential: $$\frac{e^2}{r} \rightarrow v_k = \frac{4\pi e^2}{k^2}$$

- Sum rules: $$\lim_{k\rightarrow 0} S(k) = \frac{\hbar k^2}{2m\omega_p}$$

$\omega_p = \sqrt{n v_k k^2/m}$ (plasma frequency)

Size corrections for potential energy:

$$V_\infty - V_N = \int_0^{2\pi/L} \frac{d^3k}{(2\pi)^3} v_k S(k) \rightarrow \frac{\omega_p}{4N}$$

What is with kinetic energy?

Thermodynamic limit extrapolation: Kinetic Energy - Shell effects and Coulomb singularity

- Coupling constant integration:

kinetic and potential energy corrections strongly related!

$$E = \int_0^{e^2} \frac{d\tilde{e}^2}{\tilde{e}^2} V(\tilde{e}) \qquad V(\tilde{e}) = \frac{1}{2\mathcal{V}} \sum_{\mathbf{k}} \frac{4\pi\tilde{e}^2}{k^2} S(k;\tilde{e}^2)$$

- Analyze wave function:

$$\Psi = \det_{i\mathbf{k}} \varphi_{\mathbf{k}}(\mathbf{r}_i) \exp\left[-\frac{1}{2}\sum_{\mathbf{k}} u_k \rho_{-\mathbf{k}} \rho_{\mathbf{k}}\right]$$

$\varepsilon_{\mathbf{k}} \leq \varepsilon_{k_F}$

Twist**A**veraged**B**oundary**C**onditions ⇔ k-point average

GC -TABC: impose Fermi surface (N varies)

long range Jastrow potential

$u_k \propto \frac{1}{k^2}$

⇒kinetic energy corrections

- general analysis (RPA): M.H., B. Bernu, D. Ceperley, J. Phys.: Conf. Ser. **321** 012020 (2011)

Correcting Finite size errors:

3DEG:
r_s=10

total energy E/N

atomic hydrogen:
metallic, BCC, r_s=1.31

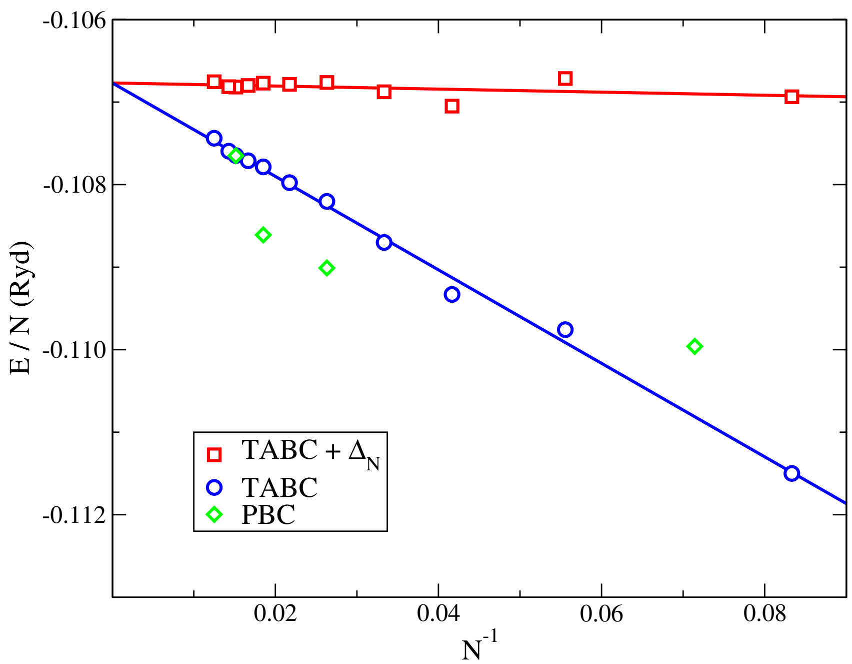

FIG. 2 (color online). Electron gas variational energies per particle at $r_s = 10$ using periodic boundary condition (PBC) and twist-averaged boundary condition (TABC). $\Delta_N \equiv \Delta T_N + \Delta V_N = \hbar\omega_p/2N$ (see text for the definition of ΔT_N and ΔV_N). Error bars are smaller than symbol size.

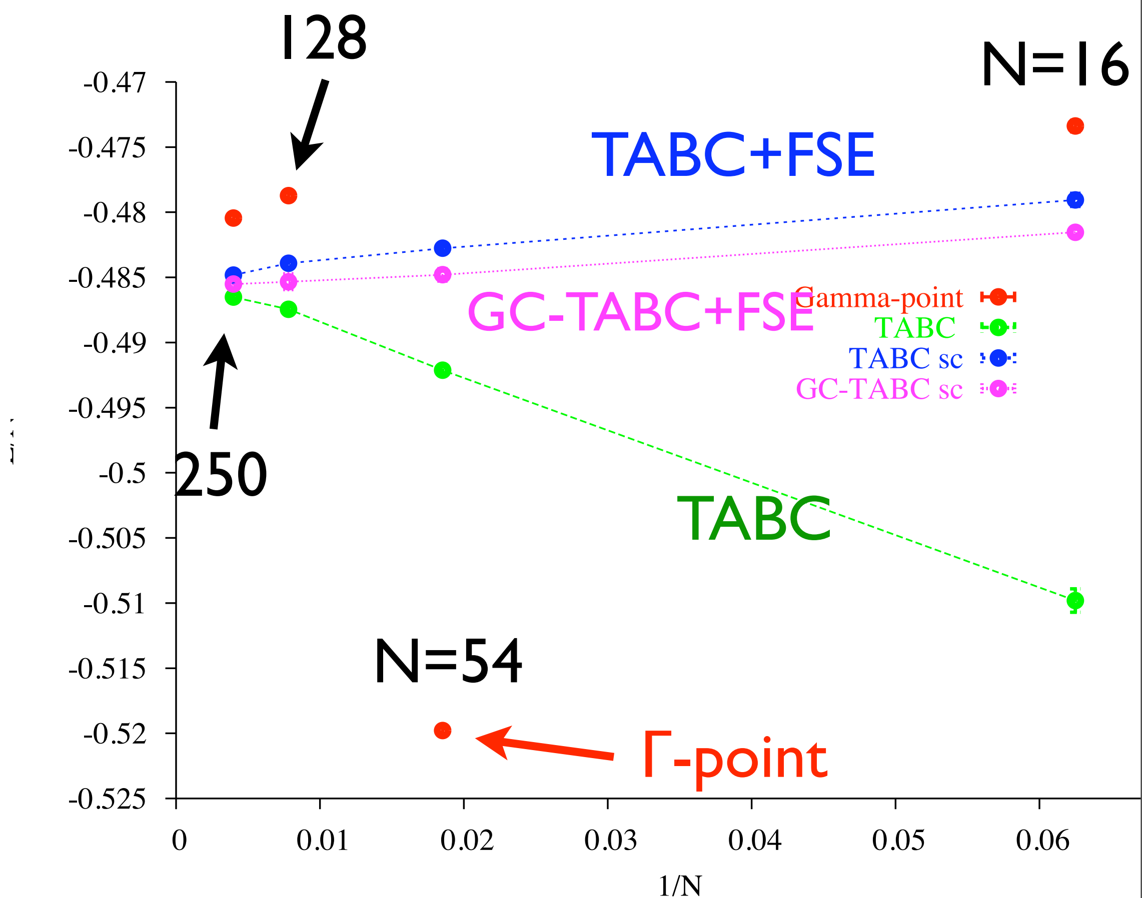

virial theorem ⇒ pressure corrections!

Momentum distribution n(k): Periodic vs Twist Averaged Boundary Conditions

GC: Grand canonical twist averaging (k-point sampling)

Slater det. with plane-wave occupation up to k_F for each twist

momentum distribution:

$$n_k \sim \int d\mathbf{r}_1 \int d\mathbf{r}_1' e^{i\mathbf{k}\cdot(\mathbf{r}_1-\mathbf{r}_1')}\Psi_T^*(\mathbf{r}_1',\ldots\mathbf{r}_N)\Psi_T(\mathbf{r}_1,\ldots\mathbf{r}_N)$$

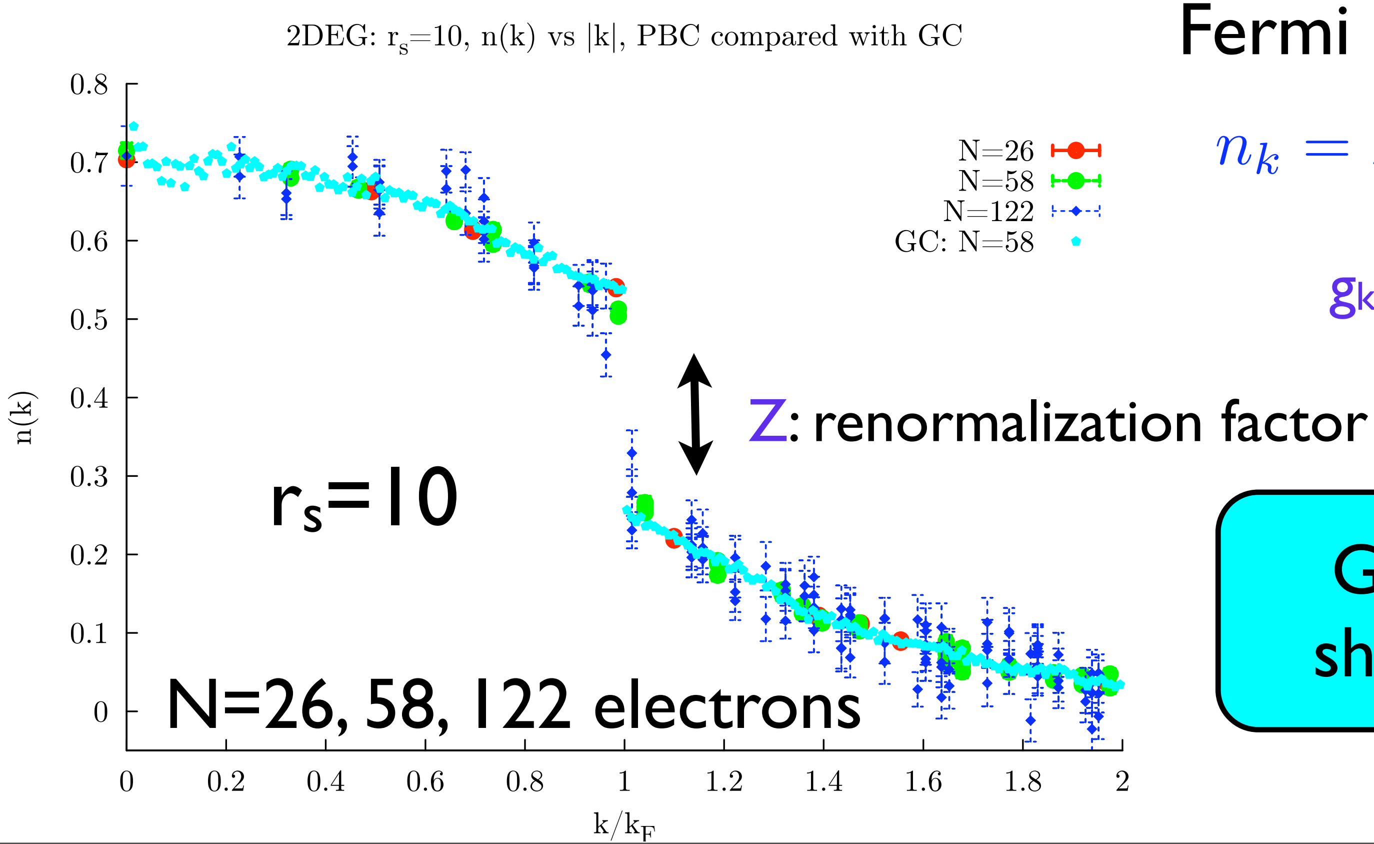

Fermi liquid structure:

$$n_k = Z\theta(k_F - |\mathbf{k}|) + g_{\mathbf{k}}$$

g_k: continuous function

GC eleminates shell oscillations

Momentum distribution n(k) (2DEG)

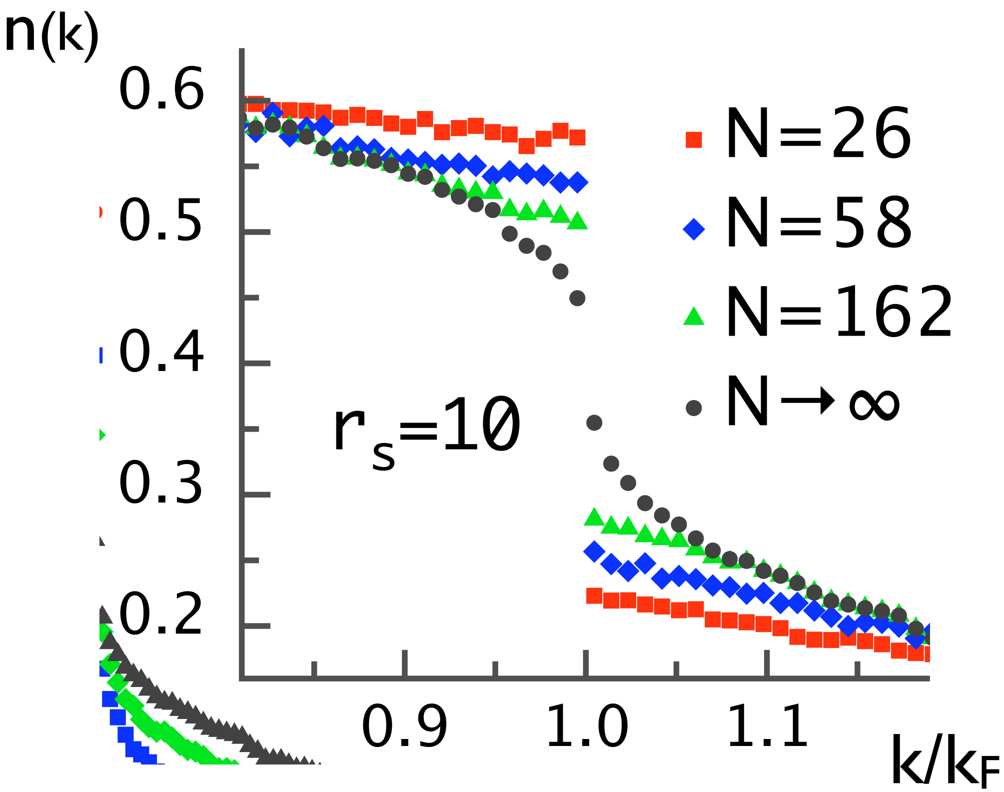

$n(k \approx k_F)$: strong size effects!

Theory of finite size effects:

$$\Psi_N \sim D_N \exp[-\textstyle\sum_k u_k \rho_k \rho_{-k}] \longrightarrow \Psi_\infty \sim D_\infty \exp[-\textstyle\int dk\, u_k \rho_k \rho_{-k}]$$

Slater determinant:
single particle modes

Jastrow potential:
collective modes

neglect mode-coupling (RPA):
analytical extrapolation for N=∞ possible

(exact for longrange properties)

Renormalization factor Z (2DEG): jump at k_F: correcting size effects

M.H., B. Bernu, V. Olevano, R.M. Martin, D.M. Ceperley, Phys. Rev. B 79, 041308(R) (2009) .

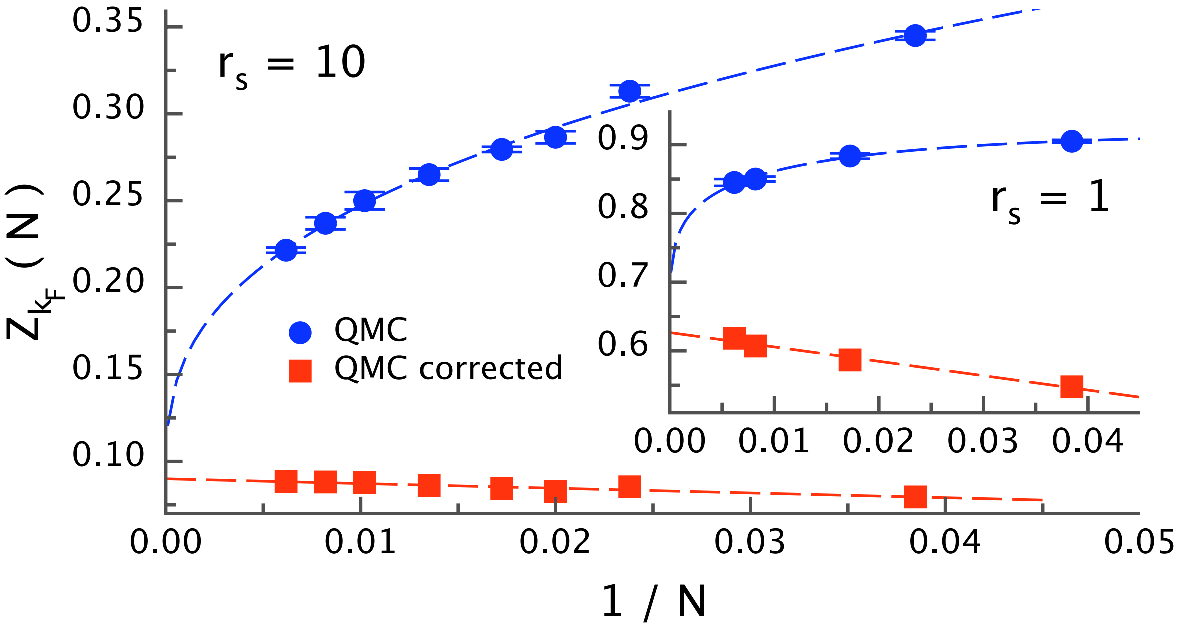

finite size correcions:

$$Z_{k_F}^{\infty} \simeq Z_{k_F}^{N} e^{-\Delta_N}$$

leading order explicitly given:

$$\Delta_N \simeq \left(\frac{\pi r_s^2}{4N}\right)^{1/4}$$

(agrees with integration error of RPA formulas)

See also:

N.D. Drummond and R.J. Needs, Phys. Rev. B 80, 245104 (2009)

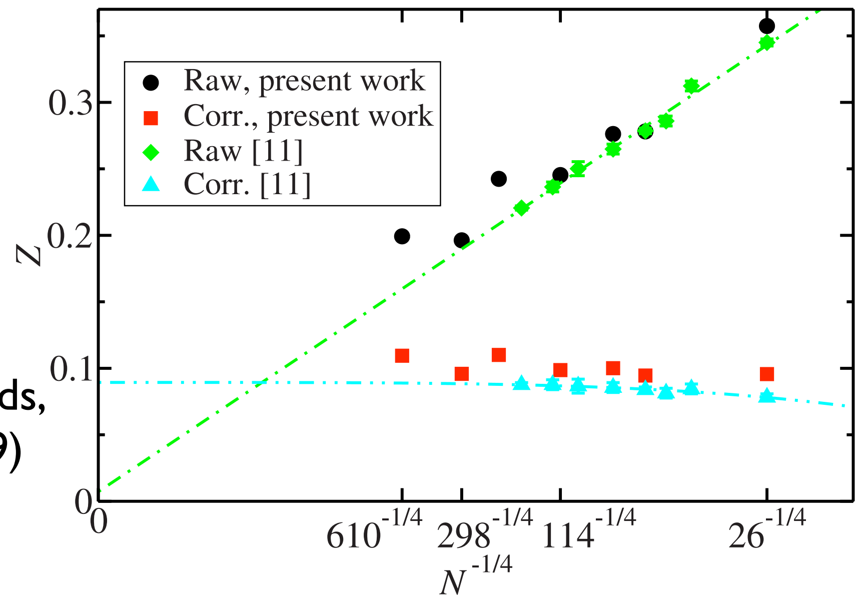

FIG. 10. (Color online) VMC renormalization factor Z against number of electrons N for paramagnetic 2D HEGs at r_s=10 a.u.

Effective mass m* (2DEG)

single particle/ hole excitations with momentum k and energy E_k

energy differences at k_F gives effective mass m*:

$$E_k - \frac{k^2}{2m} = 2k_F\left(\frac{m}{m^*} - 1\right)(k - k_F) + \dots$$

non-analytic (log) behavior expected

big size effects, similar to Z, but more difficult!

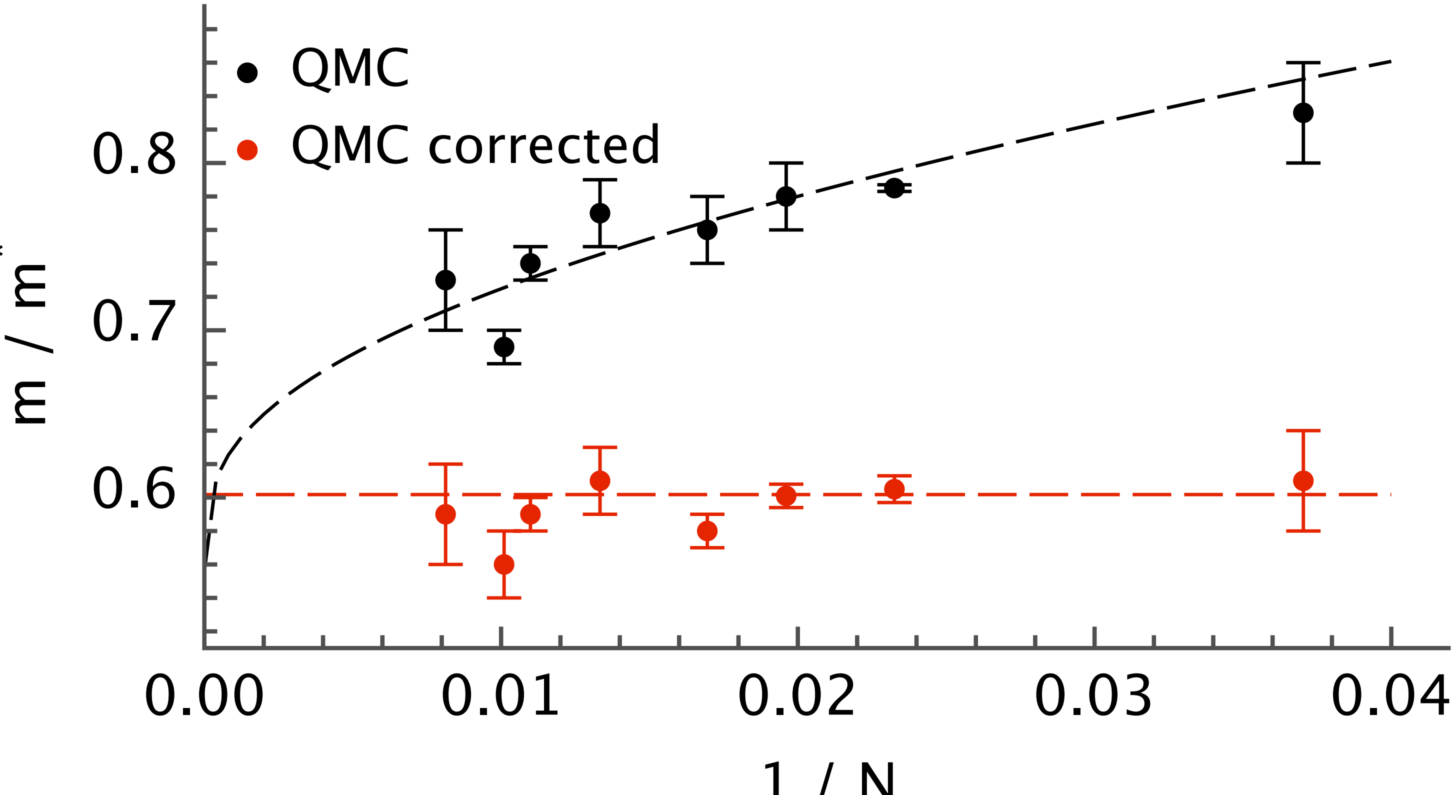

2 extrapolations:

- $N \to \infty$
- $k \to k_F$

≡ 2 major difficulties !

Effective mass m* and Z in thermodynamic limit comparision with RPA theories (2DEG)

M.H., B. Bernu, V. Olevano, R.M. Martin, D.M. Ceperley, Phys. Rev. B 79, 041308(R) (2009) .

Z vs r_s

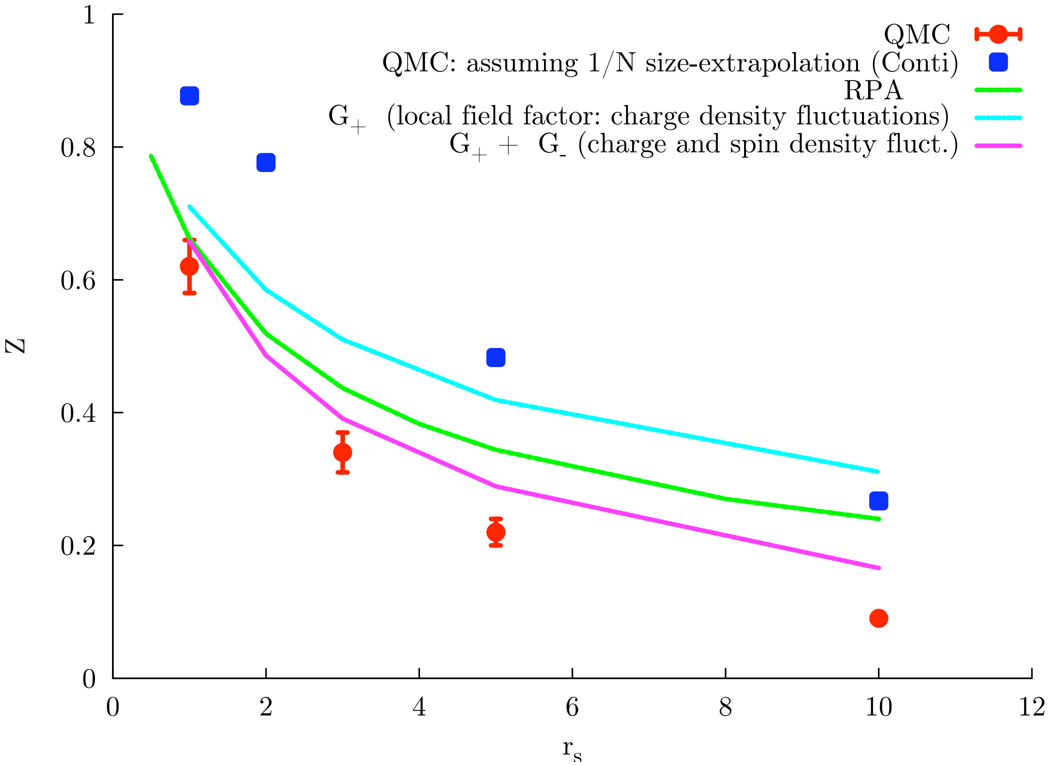

m*/m vs r_s

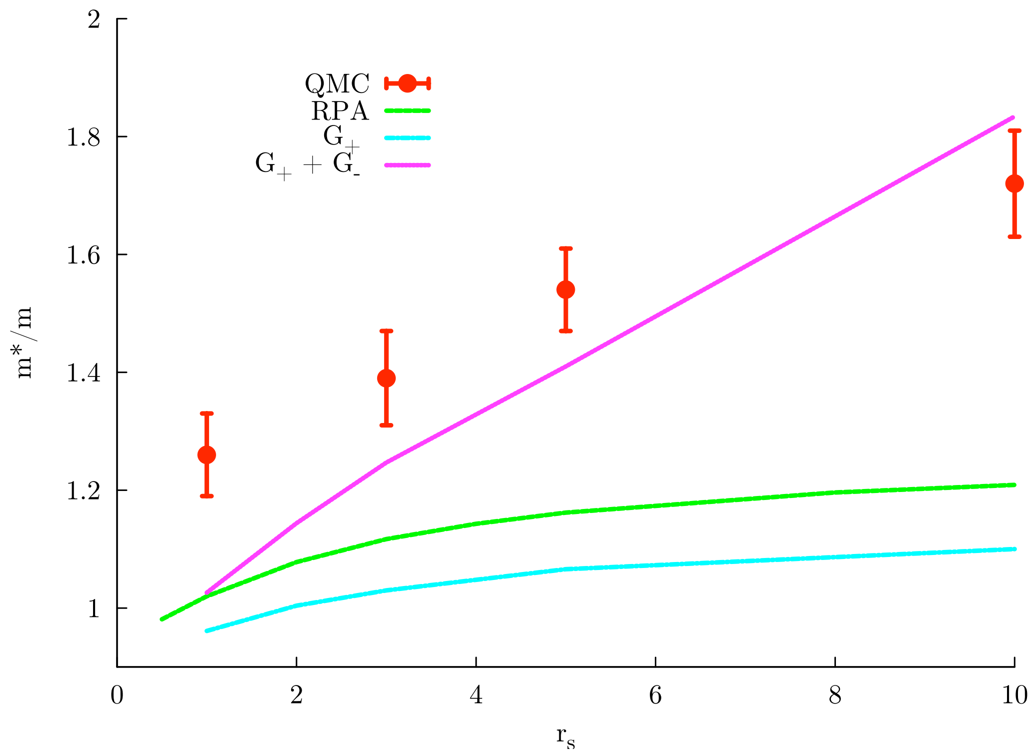

RPA: H.-J. Schulze, P. Schuck, and N. Van Giai, Phys. Rev. B 61, 8026 (2000)

G+,G-: R. Asgari, B. Davoudi, M. Polini, G. Giuliani, M. Tosi, G. Vignale, Phys.Rev. B 71, 045323 (2005).

disagreement for m* with N.D. Drummond and R.J. Needs, Phys. Rev. B 80, 245104 (2009) and PRB 87, 045131 (2013)

Imaginary Time Dynamics: Density Fluctuations

$$S(\mathbf{k},\tau) = \langle \Psi_0 | \rho_{-\mathbf{k}} \boxed{e^{-\tau(H-E_0)}} \rho_{\mathbf{k}} | \Psi_0 \rangle$$

dynamic structure factor

$$= \int_{-\infty}^{\infty} d\omega \, e^{-\tau\omega} S(\mathbf{k},\omega)$$

Imaginary time correlations:

Usual fixed-node propagator (static nodes) gives wrong dynamics

Use restricted path integral representation:

Correct dynamics if time-dependent nodes correct

Imaginary Time Dynamics: TEST
Ideal Fermi gas

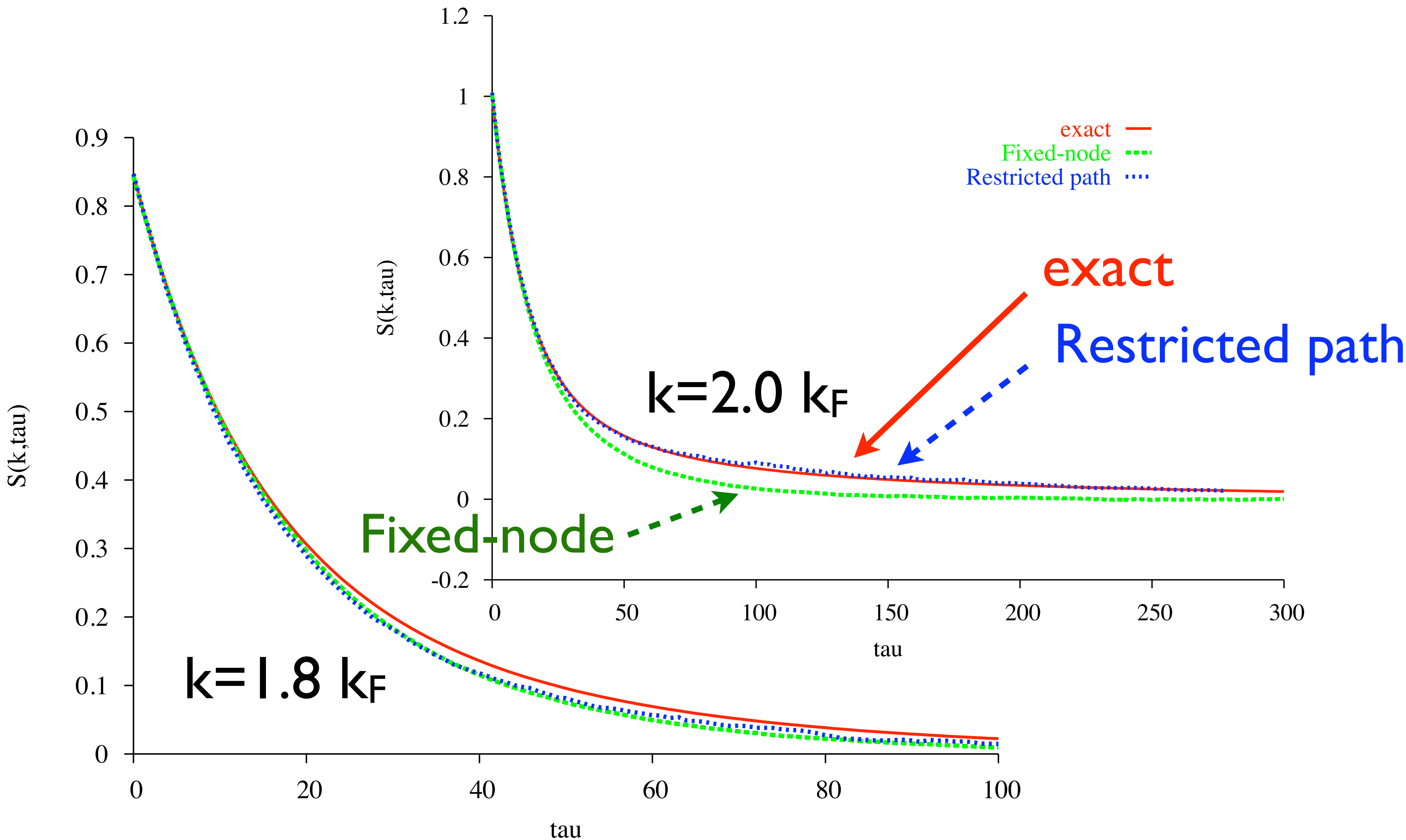

Imaginary Time Dynamics (2DEG): Plasmon Excitations

M.H., S. Moroni

2D electron gas: r_s=10 (N=26):

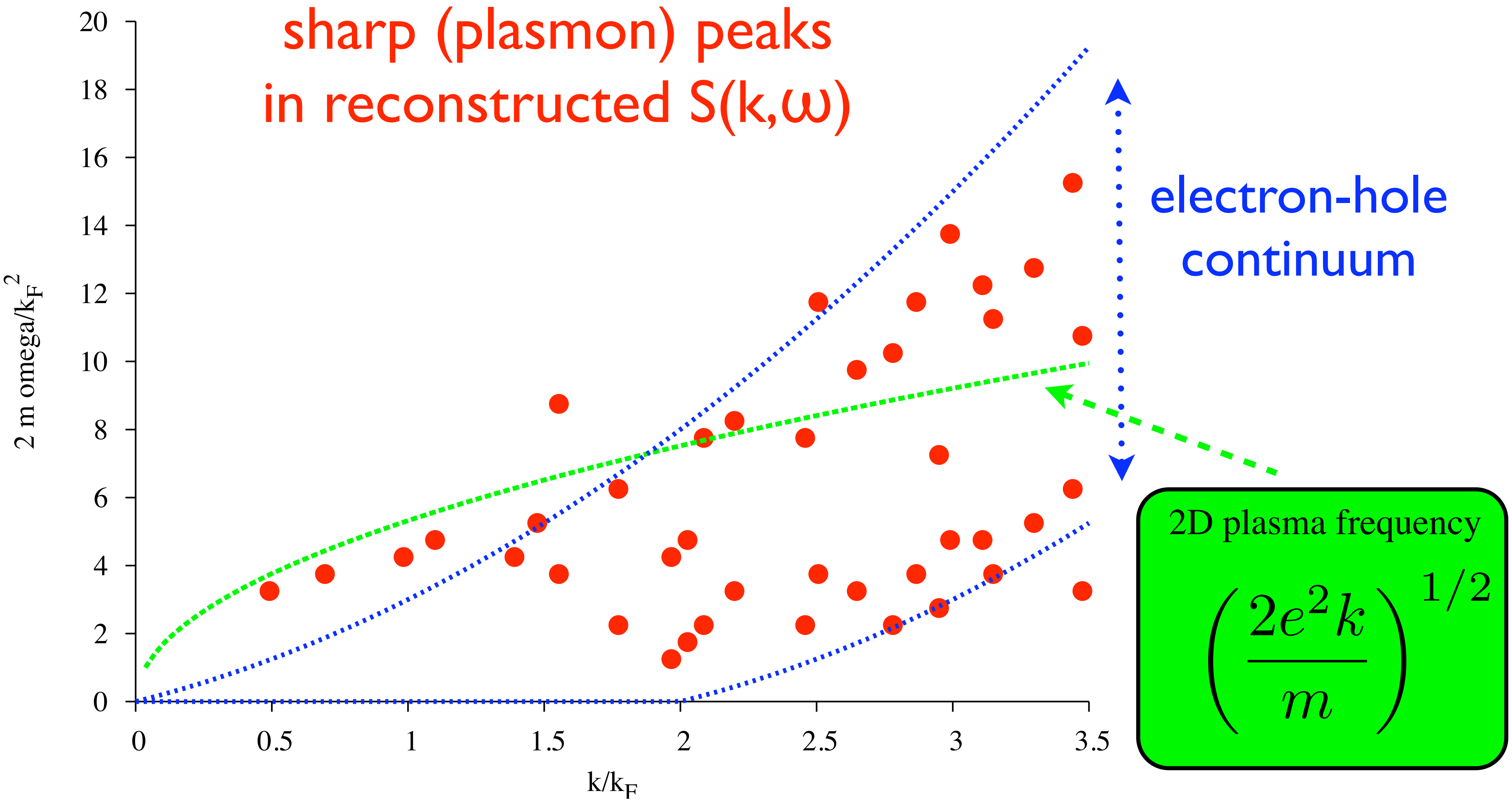

n(k), Z of jellium (3DEG) at various densities

M.H., B. Bernu, C. Pierleoni, J. McMinis, D.M. Ceperley,V. Olevano, L. Delle Site, PRL **107**, 110402 (2011) (2011).

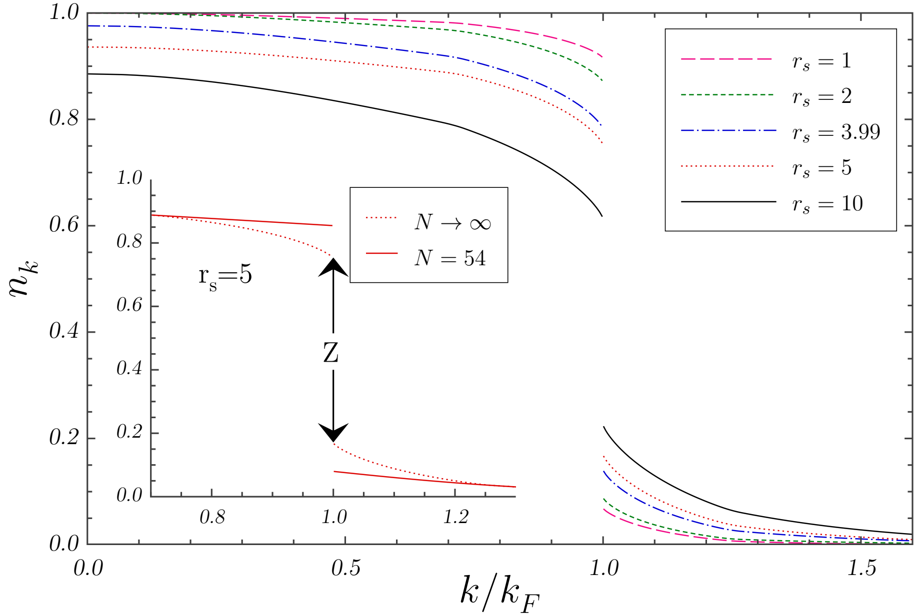

from analytical expressions of Ψ:
exact behavior of n_k around k_F

Quantitative agreement of QMC with G_0W_0 over broad density region $1 \le r_s \le 5...10$)

r_s	1	2	3.99	5	10
BF-RMC	0.84(2)	0.77(1)	0.64(1)	0.58(1)	0.40(1)
SJ-VMC	0.894(9)	0.82(1)	0.69(1)	0.61(2)	0.45(1)
BF-VMC	0.86(1)	0.78(1)	0.65(1)	0.59(1)	0.41(1)
G_0W_0 [25]	0.859	0.768	0.646*	0.602	0.45
GW_0 [26]		0.804	0.702*		
GW [27]		0.846	0.793*		
Lam [28]	0.896	0.814	0.615*	0.472	
RPA[28]	0.843	0.700	0.442*	0.323	
SJ-DMC [6]	0.952	0.889		0.725	0.593

renormalization factor Z

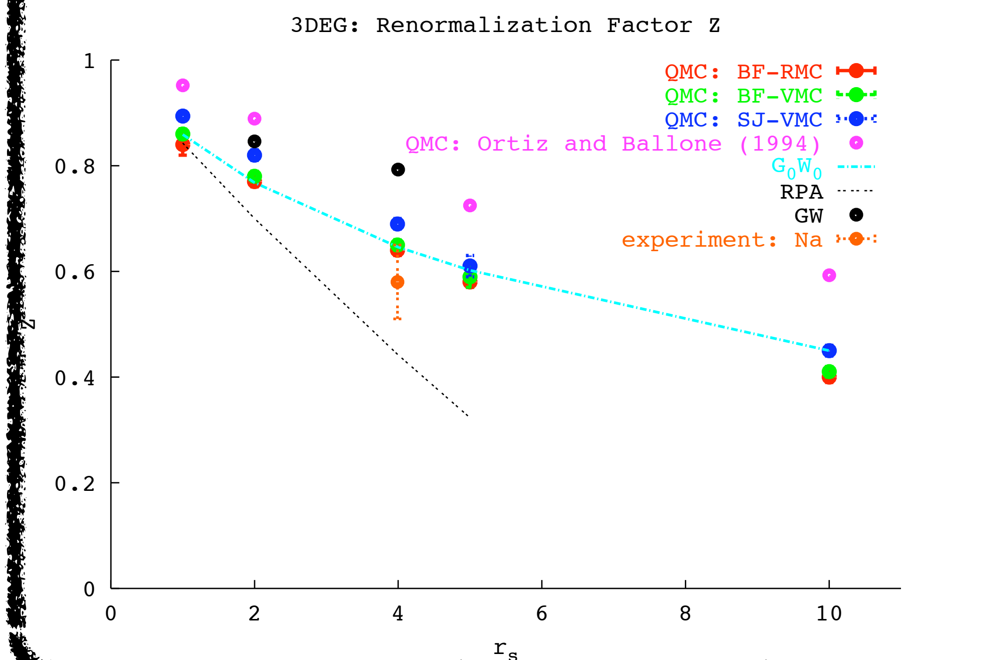

[25] L. Hedin, Phys.Rev. 139, A796 (1965).
[26] U. von Barth, B. Holm, PRB 54, 8411 (1996).
[27] B. Holm, U. von Barth, PRB 57, 2108 (1998).
[28] J. Lam, PRB 3, 3243 (1971).
[6] G. Ortiz, P. Ballone, PRB 50, 1391 (1994).

Momentum distribution of Jellium (3DEG) and sodium: G_0W_0, QMC, experiment...

S. Huotari, J. A. Soininen, T. Pylkkänen, A. Titov, A. Issolah, K. Hämäläinen, J. McMinis, J. Kim, K. Esler, D.M. Ceperley, M. H., and V. Olevano, Phys. Rev. Lett. 105, 086403 (2010).

valence electrons in Na ≈ 3DEG

- Na: very isotropic valence band
- spherical Fermi surface: anisotropies around k_F <≈0.2%

momentum distribution can be measured
via inelastic X-ray scattering
(Compton profile)

Compton profile from inelastic X-ray scattering

scattering cross section:

high energies (synchrotron): impulsive approximation

$$\frac{d^2\sigma}{d\Omega d\omega_2} = \left(\frac{d\sigma}{d\Omega}\right)_{Th} S(\mathbf{k},\omega)$$

$$S(\mathbf{k},\omega) \simeq J_{\hat{\mathbf{k}}}\left(\omega/k - k/2\right)$$

dynamic structure factor

Compton profile $J_{\mathbf{k}}(q) = \int d^3\mathbf{p}\, n(\mathbf{p})\delta(\mathbf{p}\cdot\hat{\mathbf{k}} - q)$

spherical averaged Compton profile

$$J(q) = \int_{|q|}^{\infty} d^2\mathbf{p}\, n(\mathbf{p})$$

momentum distribution n(k) by differentiation

renormalization factor Z gives kink

Valence electron Compton profile of Na: experiment

subtract contribution of core electrons

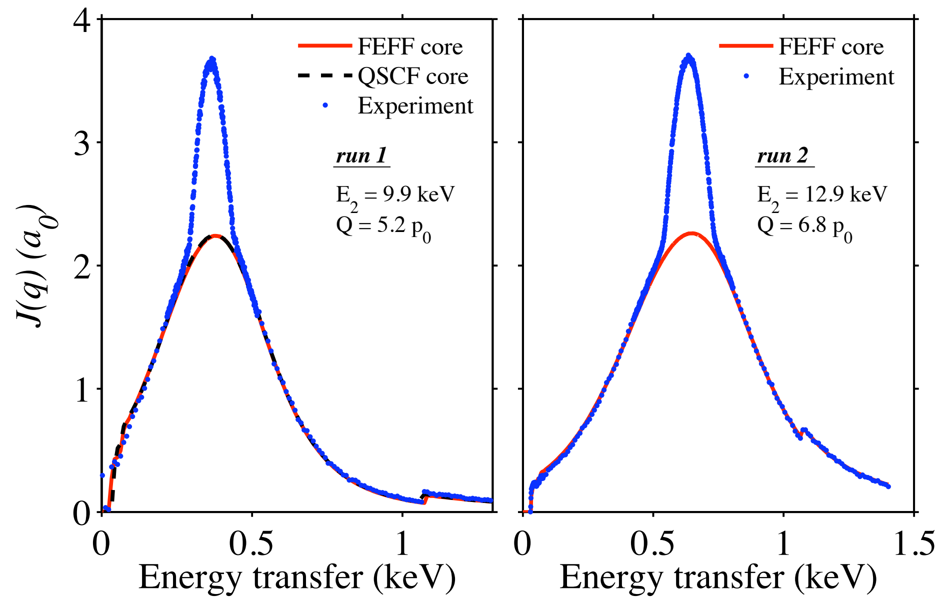

FIG. 2 (color online). The measured x-ray-scattering spectra from Na as a function of energy transfer, for both experimental runs. The experimental spectra consist of overlapping valence and core contributions. Theoretical core contributions are shown for both QSCF and FEFFQ treatments.

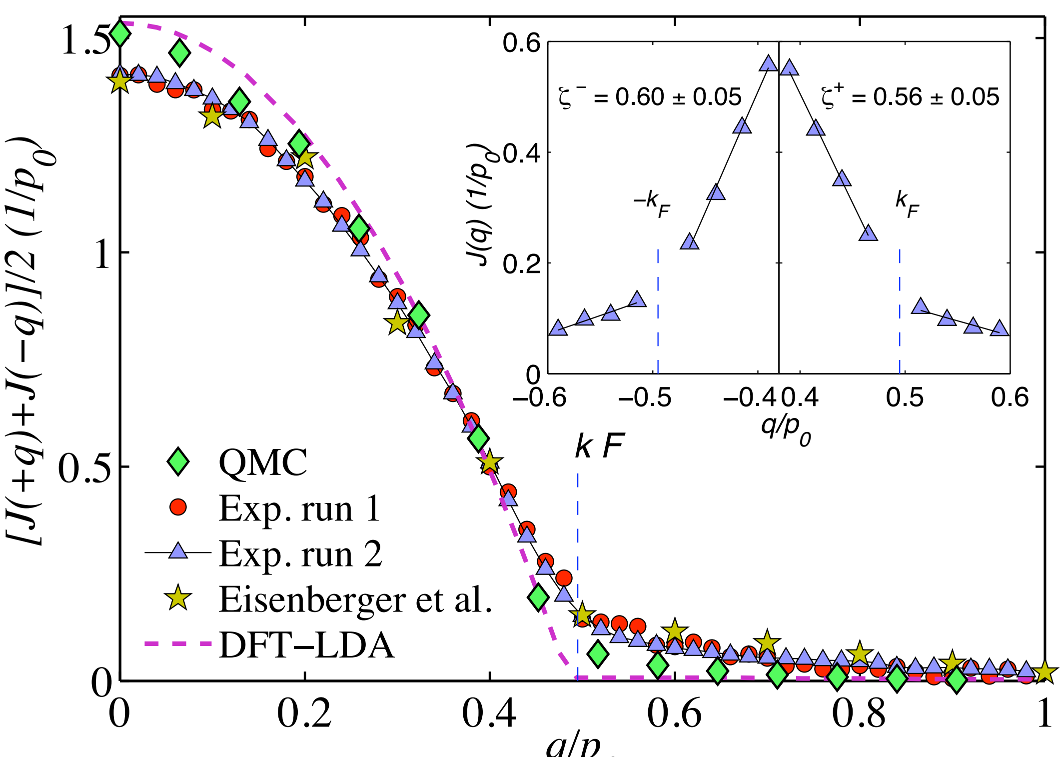

discontinuity in the slope at k_F: direct measurement of Z and k_F

momentum distribution of Na
renormalization factor Z of 3DEG at r_s=3.99

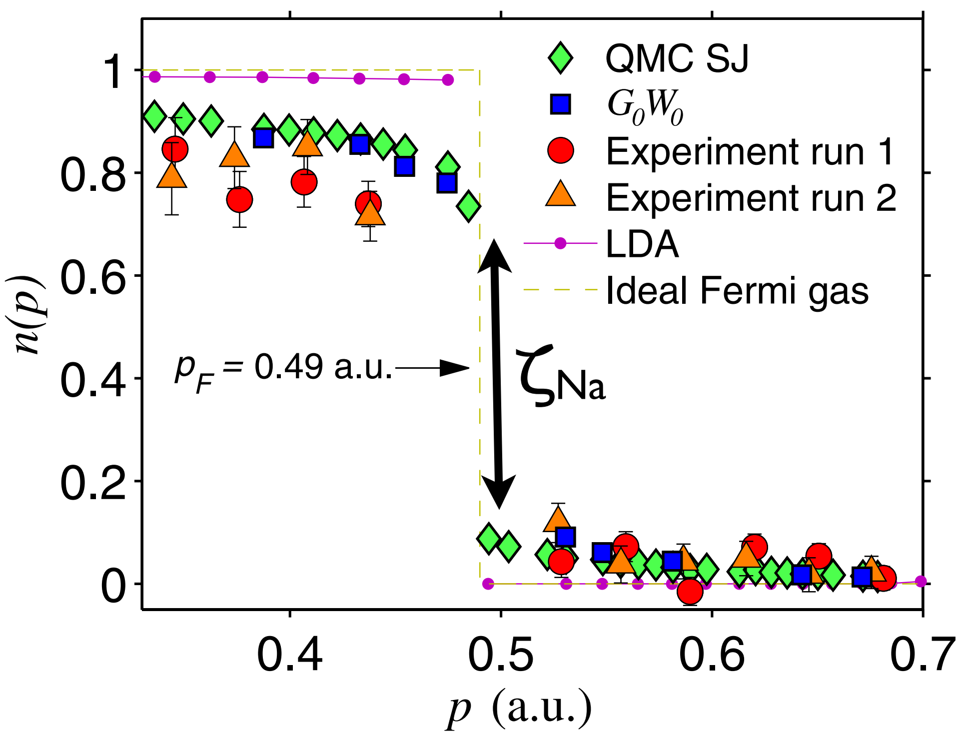

FIG. 1 (color online). The momentum distribution of Na determined by experiment, QMC SJ, G_0W_0, and LDA calculations. The ideal-Fermi gas step function is also shown.

valence electron density:
r_s=3.99

QMC and G_0W_0 indicate
that bandstructure and correlation effects
factorize at k_F

$$\zeta_{\mathrm{Na}} = |\tilde{\phi}^{\mathbf{G}=0}_{\nu=1,\mathbf{k}_F}|^2 Z_{\mathbf{k}_F}$$

LDA bandstructure wfn-coeff. $Z_{Na} \cong Z_{3DEG}$

Technique	ζ^{Na}	$Z^{\mathrm{Na}}_{k_F}$	$Z^{\mathrm{HEG}}_{k_F}$
Experiment	0.57(7)	0.58(7)	
QMC SJ	0.68(2)	0.70(2)	0.69(1)
QMC BF			0.66(2)
G_0W_0	0.64(1)	0.65(1)	0.64 [2]
GW [6]			0.793
RPA (on shell)			0.45
$\exp S_2$ [4]			0.59
EPX [8]			0.61
Lam [5]			0.615
FHNC [7]			0.71

comparision with theories

Summary and Outlook

- QMC-calculations of E, n(k), Z, m*, ... :

  Importance of thermodynamic limit extrapolation

- QMC calculation of m* for the 3DEG, Na, ...

- Differences in Compton profile of sodium:
  Final state effects, core electrons, phonons?

- Imaginary time dynamics:

  Spectral properties, conductivity, ...

B. Bernu, D. Ceperley, S. Chiesa, K. Esler, J. McMinis,
J. Kim, S. Moroni, V. Olevano,...